

510 mg, 1.27 mmol, 95.5%): mp 95 °C, IR (Nujol) 1125, 1015, 1000, 840, 315 cm⁻¹; ¹H NMR (300 MHz, CDCl₃) δ 1.39 (d, 6 H), 2.05 (m, 8 H), 4.37 (m, 8 H), 4.66 (septet, 1 H). Anal. Calcd for C₁₁H₂₃Cl₃O₃Zr: C, 32.95; H, 5.79. Found: C, 31.21; H, 5.62.

Preparation of the 1:4 Tetrahydrofuran Adduct of Bidentate Zirconium Trichloride Alkoxide 8. A stirred solution of the 1:2 tetrahydrofuran adduct 3^{2b} of ZrCl₄ (600 mg, 1.59 mmol) in dichloromethane (2 mL) was treated dropwise at 25 °C under dry N₂ with a solution of the bis(trimethylsilyl) ether ⁷10 of racemic *trans*-1,2-cyclohexanediol (207 mg, 0.795 mmol) in dichloromethane (1 mL). The resulting mixture was stirred at 25 °C for 24 h and filtered into a test tube. A layer of pentane (3 mL) was carefully added, and the tube was kept at -25 °C for several days. This produced a crop of colorless needles contaminated with a small amount of white powder. The crystals were separated mechanically and shown by X-ray crystallography to be a 1:1 dichloromethane solvate of the 1:4 tetrahydrofuran adduct of bidentate zirconium alkoxide 8 (400 mg, 0.453 mmol, 57.0%): mp 86-88 °C; IR (Nujol) 1160, 1090, 990, 830, 730, 315 cm⁻¹. Anal. Calcd for C₂₂H₄₂Cl₆O₆Zr₂·CH₂Cl₂: C, 31.29; H, 5.03. Found: C, 30.29; H, 4.97.

Crystallographic Data for the 1:4 Tetrahydrofuran Adduct of Bidentate Zirconium Trichloride Alkoxide 8. Crystals suitable for an X-ray study were grown by crystallization from dichloromethane/pentane. The sample selected for analysis had the following dimensions: 0.27 × 0.35 × 0.39 mm. Other crystallographic data are summarized in Table I.

Crystallographic Measurements and Structure Resolution. An Enraf-Nonius CAD-4 diffractometer was used to collect a set of intensity data according to a procedure described elsewhere.¹⁴ Seven standard reflections checked every 1 h showed random fluctuations of less than ±3.0% about their respective means. A set of 14518 Mo Kα reflections (2θ ≤ 50°) was collected at 220 K over half the Laue sphere (±h, ±k, ±l). Of these, 3699 (I ≤ 3σ(I)) were retained for structure resolution and refinement after averaging to Laue 2/m symmetry. These measurements were corrected for the Lorentz effect and polarization but not

(14) Bélanger-Gariépy, F.; Beauchamp, A. L. *J. Am. Chem. Soc.* **1980**, *102*, 3461-3464.

for absorption. The structure was solved by using direct methods (EEMS) and difference-Fourier calculations (SHELX), and it was refined on |F_o| by full-matrix least-squares procedures. All non-hydrogen atoms were refined anisotropically. For disordered CH₂Cl₂, occupancies were initially refined by using common isotropic temperature factors, and then the occupancies were fixed and anisotropic temperature factors were used. Refinement converged to R = 0.042 and R_w = 0.042, and the goodness-of-fit ratio S was 1.88 for 407 parameters refined. The final ΔF map was essentially featureless, with a general background below ±0.20 e Å⁻³, seven peaks of 0.25-0.37 e Å⁻³ within 0.94 Å from Zr, and four peaks of 0.21-0.23 e Å⁻³ within 1.2 Å from Cl. The scattering curves for the non-hydrogen atoms¹⁵ and hydrogen atoms¹⁶ were taken from standard sources. Contributions of Zr and Cl to anomalous dispersion were included.¹⁷

Selected interatomic distances and bond angles are listed in Table II, and atomic coordinates and isotropic temperature factors are provided in Table III. Tables of anisotropic temperature factors and structure factors are included as supplementary material.

Acknowledgment. This work was funded by the Natural Sciences and Engineering Research Council of Canada, by the Ministère de l'Éducation du Québec, and by Merck Frost. In addition, we are grateful to Sylvie Bilodeau of the Regional High-Field NMR Laboratory for helping us record our low-temperature ¹H NMR spectra.

Supplementary Material Available: For the 1:4 tetrahydrofuran adduct of bidentate zirconium trichloride alkoxide 8, Table SI, containing anisotropic temperature factors (2 pages); Table SII, containing structure factors (24 pages). Ordering information is given on any current masthead page.

(15) Cromer, D. T.; Waber, J. T. *Acta Crystallogr.* **1965**, *18*, 104-109.

(16) Stewart, R. F.; Davidson, E. R.; Simpson, W. T. *J. Chem. Phys.* **1965**, *42*, 3175-3187.

(17) Cromer, D. T.; Liberman, D. *J. Chem. Phys.* **1970**, *53*, 1891-1898.

Contribution from the Department of Chemistry,
Texas A&M University, College Station, Texas 77843-3255

New Low-Dimensional Zinc Compounds Containing Zinc-Oxygen-Phosphorus Frameworks: Two-Layered Inorganic Phosphites and a Polymeric Organic Phosphinate

Minghuy Shieh, Kevin J. Martin, Philip J. Squattrito, and Abraham Clearfield*

Received June 12, 1989

Two new zinc phosphites have been prepared by reaction of zinc chloride with either calcium or strontium phosphite in aqueous phosphorous acid. The compounds have been characterized by single-crystal X-ray diffraction techniques. ZnCa(HPO₃)₂(H₂O)₂: P2₁/n, a = 7.131 (2) Å, b = 7.766 (2) Å, c = 14.479 (2) Å, β = 97.30 (2)°, V = 795.3 (3) Å³, Z = 4, R(F_o) = 0.045 for 1063 observations (I > 3σ(I)) and 109 variables. ZnSr(HPO₃)₂(H₂O)₂: P1̄, a = 7.728 (2) Å, b = 7.967 (2) Å, c = 7.448 (2) Å, α = 99.56 (2)°, β = 107.93 (2)°, γ = 100.51 (2)°, V = 416.6 (2) Å³, Z = 2, R(F_o) = 0.034 for 1187 observations (I > 3σ(I)) and 109 variables. Both compounds have layered structures in which the zinc atoms are tetrahedrally coordinated and the Ca or Sr atoms are 8-coordinate. In each case, the interlayer region is lined with water molecules coordinated to the alkaline-earth-metal ion. The modes in which Ca and Sr bridge the phosphite groups are different, however, resulting in layers with different topographies. These results, together with earlier work on Na⁺, K⁺, and Ba²⁺, are discussed in terms of the effect of the alkali or alkaline-earth metals on the observed structural trends. A new polymeric zinc phenylphosphinate has also been synthesized and its structure determined. Crystal data for Zn(O₂PHC₆H₅)₂: C2/c, a = 15.763 (2) Å, b = 11.162 (2) Å, c = 8.272 (2) Å, β = 109.34 (2)°, V = 1373.2 (6) Å³, Z = 4, R(F_o) = 0.047 for 480 observations (I > 3σ(I)) and 105 variables. The structure is compared with known phosphinates and phosphonates.

Introduction

As an outgrowth of our continuing interest in transition-metal phosphates with framework structures,^{1,2} we recently reported the synthesis of a novel series of zinc phosphites containing alkali or alkaline-earth metals.³ Each of the compounds prepared (containing Na⁺, K⁺, and Ba²⁺, respectively) had a different structure that was highly dependent on the coordination requirements of

the alkali- or alkaline-earth-metal ion. In order to further examine the structural trends in these materials, we have prepared and characterized two new zinc phosphites of calcium and strontium. In addition, we have been exploring the chemistry of organic derivatives⁴⁻⁷ of layered transition-metal phosphates and recently

* To whom correspondence should be addressed.

(1) Clearfield, A. *Chem. Rev.* **1988**, *88*, 125-148 and references therein.

(2) *Inorganic Ion Exchange Materials*; Clearfield, A., Ed.; CRC Press: Boca Raton, FL, 1982.

(3) Ortiz-Avila, C. Y.; Squattrito, P. J.; Shieh, M.; Clearfield, A. *Inorg. Chem.* **1989**, *28*, 2608-2615.

described several new phosphonates⁸ and organic phosphates⁹ of zinc. Of late, these studies have been extended to the corresponding phosphinates. We report here the synthesis and structure of zinc phenylphosphinate, $\text{Zn}(\text{O}_2\text{PHC}_6\text{H}_5)_2$, and the phosphites $\text{ZnCa}(\text{HPO}_3)_2(\text{H}_2\text{O})_2$ and $\text{ZnSr}(\text{HPO}_3)_2(\text{H}_2\text{O})_2$. These results are discussed in the context of our earlier findings.

Experimental Section

Syntheses. $\text{ZnCa}(\text{HPO}_3)_2(\text{H}_2\text{O})_2$. A 0.67-g sample of ZnCl_2 (Mallinckrodt reagent grade, used as received) was added to a solution of 1.20 g of $\text{CaHPO}_3 \cdot \text{H}_2\text{O}$ (prepared from $\text{Ca}(\text{OH})_2$ and H_3PO_3 according to ref 10) in 10 mL of aqueous 1 M H_3PO_3 (Aldrich, 99%). The clear solution was stirred overnight, followed by the addition of 7 mL of EtOH. Colorless platelike crystals suitable for X-ray analysis were obtained after the solution had been allowed to stand for several days at room temperature. A thermogravimetric analysis of the sample was performed on a Cahn RH electrobalance. The observed weight loss (onset, 130 °C; completion, 310 °C) of 11.94% is consistent with loss of 2 mol of water per formula unit (calculated 11.95%).

$\text{ZnSr}(\text{HPO}_3)_2(\text{H}_2\text{O})_2$. A 0.67-g sample of ZnCl_2 was added to a solution of 1.67 g of $\text{SrHPO}_3 \cdot \text{H}_2\text{O}$ (prepared from SrCO_3 and H_3PO_3 as described in ref 10) in 12 mL of aqueous 1 M H_3PO_3 . The resultant solution was stirred for 2 days, after which 3 mL of EtOH was added. Small colorless platelets grew from the solution, which was allowed to stand at room temperature for 10 days. A TGA of the crystals showed a weight loss of 10.18% between 30 and 290 °C (calculated for $\text{ZnSr}(\text{HPO}_3)_2(\text{H}_2\text{O})_2$ on the basis of H_2O 10.32%).

$\text{Zn}(\text{O}_2\text{PHC}_6\text{H}_5)_2$. A 10-mL aliquot of 1 M ZnCl_2 solution (0.01 mol) was added to 1.4 g of $\text{HO}_2\text{PHC}_6\text{H}_5$ (phenylphosphinic acid) (0.01 mol) in 50 mL of aqueous 30% EtOH. A polycrystalline white solid precipitated immediately. An X-ray powder diffraction pattern of the sample is in excellent agreement with that calculated from the single-crystal structure of $\text{Zn}(\text{O}_2\text{PHC}_6\text{H}_5)_2$ (vide infra). Colorless, plate-shaped crystals suitable for the single-crystal X-ray study were grown from a standing solution of 0.7 g of $\text{HO}_2\text{PHC}_6\text{H}_5$ (0.005 mol) and 5 mL of 1 M ZnCl_2 (0.005 mol) in 100 mL of water.

Crystallographic Studies. All single-crystal X-ray diffraction work was performed at room temperature on a Rigaku AFC5R four-circle diffractometer equipped with a 12-kW rotating anode Mo X-ray source ($\lambda(\text{K}\alpha) = 0.71069 \text{ \AA}$). In each case, a suitable single crystal was mounted on a glass fiber with silicone cement. Unit cell parameters were derived from least-squares refinements of the setting angles of 25 high-angle reflections ($25^\circ < 2\theta(\text{Mo K}\alpha) < 50^\circ$) in which the monoclinic cell angles α and γ were constrained to be 90° . Intensity data were collected by using the ω - 2θ scan technique at $16^\circ/\text{min}$ ($\text{Zn}(\text{O}_2\text{PHC}_6\text{H}_5)_2$) or $8^\circ/\text{min}$ ($\text{ZnCa}(\text{HPO}_3)_2(\text{H}_2\text{O})_2$ and $\text{ZnSr}(\text{HPO}_3)_2(\text{H}_2\text{O})_2$) in ω . Up to three identical scans were performed on weak data. The intensities of three standards checked at 150-reflection intervals throughout data collection displayed only small random variations. All crystallographic computations were performed on a DEC MicroVAX II computer with the TEXSAN¹¹ series of programs. Space groups were assigned on the basis of systematic absences and intensity statistics. In all cases, these led to satisfactory refinements. Each of the structures was solved by direct methods (MITHRIL¹²). The positions of the heavy atoms Zn, Ca, and Sr were taken from *E* maps, while the remaining non-hydrogen atoms were located by direct-methods phase refinement techniques (DIRDIF¹³).

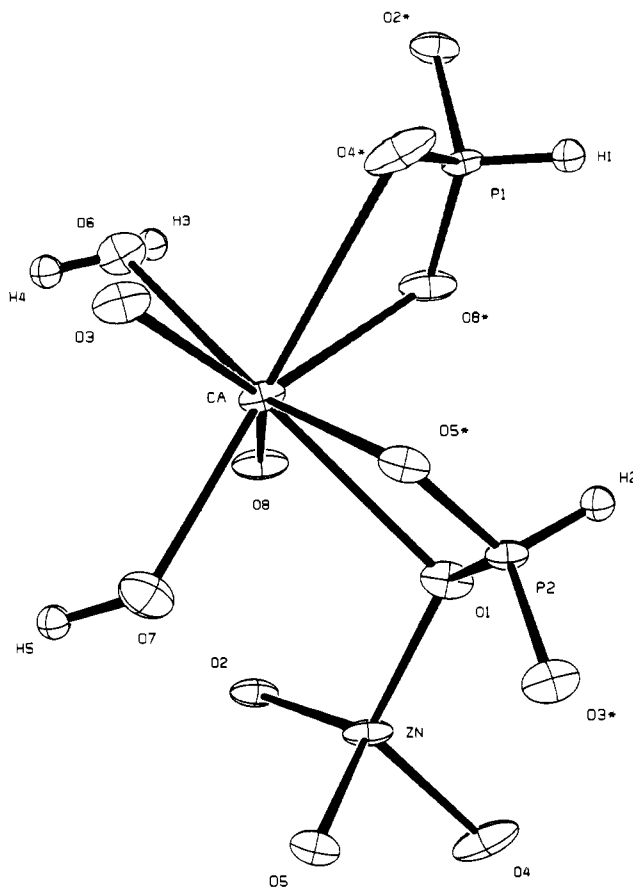


Figure 1. Connectivity of the various coordination polyhedra in $\text{ZnCa}(\text{HPO}_3)_2(\text{H}_2\text{O})_2$. Thermal ellipsoids in this and succeeding figures are shown at the 50% probability level. Hydrogen atoms are shown as isotropic spheres of arbitrary size.

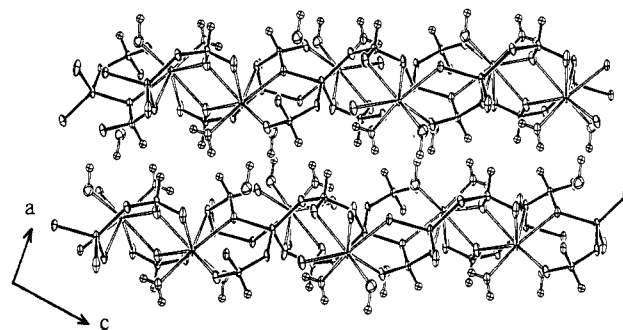


Figure 2. Perspective drawing of the $\text{ZnCa}(\text{HPO}_3)_2(\text{H}_2\text{O})_2$ structure along $[010]$, showing the layers as viewed edge-on. The bonds to zinc and phosphorus are solid black, while those to Ca are hollow.

- Alberti, G.; Allulli, S.; Costantino, U.; Tomassini, N. *J. Inorg. Nucl. Chem.* **1978**, *40*, 1113-1117.
- Cunningham, D.; Hennelly, P.; Deeney, T. *Inorg. Chim. Acta* **1979**, *37*, 95-102.
- Cao, G.; Lee, H.; Lynch, V.; Mallouk, T. *Solid State Ionics* **1988**, *26*, 63-69.
- Cao, G.; Lee, H.; Lynch, V.; Mallouk, T. *Inorg. Chem.* **1988**, *27*, 2781-2785.
- Martin, K. J.; Squattrito, P. J.; Clearfield, A. *Inorg. Chim. Acta* **1989**, *155*, 7-9.
- Ortiz-Avila, C. Y.; Rudolf, P. R.; Clearfield, A. *Inorg. Chem.* **1989**, *28*, 2137-2141.
- Mellor's Comprehensive Treatise on Inorganic and Theoretical Chemistry*; Wiley: New York, 1971; Vol. III, Suppl. III, p 641 and references therein.
- TEXSAN. *Textray Structural Analysis Package*; Molecular Structure Corp.: The Woodlands, TX, 1987 (revised).
- Gilmore, G. J. MITHRIL. A Computer Program for the Automatic Solution of Crystal Structures from X-ray Data. University of Glasgow, Scotland, 1983.
- Beurskens, P. T. DIRDIF: Direct Methods for Difference Structures—An Automatic Procedure for Phase Extension and Refinement of Difference Structure Factors. Technical Report 1984/1; Crystallography Laboratory: Toernooiveld, 6525 Ed Nijmegen, The Netherlands, 1984.

Difference electron density maps revealed the positions of all the phosphate hydrogen atoms and all but one of those in coordinated water molecules of the Ca compound. The water protons could not be located in the Sr compound, their presence probably masked by the high absorption of the material. The phenyl H atoms in $\text{Zn}(\text{O}_2\text{PHC}_6\text{H}_5)_2$ were also found via a difference Fourier synthesis and their positions refined. Final refinements for all the structures were performed on those data having $I > 3\sigma(I)$ and included anisotropic thermal parameters for all non-hydrogen atoms. Analyses of F_o vs F_c as a function of $(\sin \theta)/\lambda$, Miller indices, and F_o displayed no unusual trends. There were no peaks in the final difference electron density maps with height greater than about 3% that of the heaviest atom in any of the structures. Due to the relatively high linear absorption coefficient ($\mu = 42 \text{ cm}^{-1}$) and the anisotropic shape of the $\text{ZnCa}(\text{HPO}_3)_2(\text{H}_2\text{O})_2$ crystal (approximate dimensions $0.30 \times 0.30 \times 0.02 \text{ mm}$), the absorption effects for this compound are not negligible. In the absence of an absorption correction, the thermal ellipsoids are elongated along the stacking axis (Figure 2).

Summaries of the X-ray experiments and crystal data for the three compounds are given in Table I. Final positional and equivalent isotropic thermal parameters are listed in Table II, while selected bond distances

Table I. Crystallographic Data for New Zinc Compounds

$\text{ZnCa}(\text{HPO}_3)_2(\text{H}_2\text{O})_2$	
$a = 7.131 (2) \text{ \AA}$	space group: $P2_1/n$ (No. 14)
$b = 7.766 (2) \text{ \AA}$	$T = 23 \text{ }^\circ\text{C}$
$c = 14.479 (2) \text{ \AA}$	$\lambda = 0.71069 \text{ \AA}$
$\beta = 97.30 (2)^\circ$	$\rho_{\text{calcd}} = 2.52 \text{ g}\cdot\text{cm}^{-3}$
$V = 795.3 (3) \text{ \AA}^3$	$\mu = 41.96 \text{ cm}^{-1}$
$Z = 4$	$R(F_o) = 0.045$
fw 301.45	$R_w(F_o) = 0.058$

$\text{ZnSr}(\text{HPO}_3)_2(\text{H}_2\text{O})_2$	
$a = 7.728 (2) \text{ \AA}$	space group: $P\bar{1}$ (No. 2)
$b = 7.967 (2) \text{ \AA}$	$T = 23 \text{ }^\circ\text{C}$
$c = 7.448 (2) \text{ \AA}$	$\lambda = 0.71069 \text{ \AA}$
$\alpha = 99.56 (2)^\circ$	$\rho_{\text{calcd}} = 2.78 \text{ g}\cdot\text{cm}^{-3}$
$\beta = 107.93 (2)^\circ$	$\mu = 95.46 \text{ cm}^{-1}$
$\gamma = 100.51 (2)^\circ$	transm coeff = 0.305–1.0
$V = 416.6 (2) \text{ \AA}^3$	$R(F_o) = 0.034$
$Z = 2$	$R_w(F_o) = 0.049$
fw 348.99	

$\text{Zn}(\text{O}_2\text{PHC}_6\text{H}_5)_2$	
$a = 15.763 (2) \text{ \AA}$	space group: $C2/c$ (No. 15)
$b = 11.162 (2) \text{ \AA}$	$T = 23 \text{ }^\circ\text{C}$
$c = 8.272 (2) \text{ \AA}$	$\lambda = 0.71069 \text{ \AA}$
$\beta = 109.34 (2)^\circ$	$\rho_{\text{calcd}} = 1.68 \text{ g}\cdot\text{cm}^{-3}$
$V = 1373.2 (6) \text{ \AA}^3$	$\mu = 20.65 \text{ cm}^{-1}$
$Z = 4$	$R(F_o) = 0.047$
fw 347.55	$R_w(F_o) = 0.052$

and angles appear in Table III. Tables of crystallographic details and anisotropic thermal parameters (Table SI) and structure amplitudes (Table SII) are available as supplementary material.

Results and Discussion

$\text{ZnCa}(\text{HPO}_3)_2(\text{H}_2\text{O})_2$. The structure is shown in Figures 1 and 2. The Zn atoms are in a very regular tetrahedral coordination (Table III) of oxygen atoms supplied by four different phosphite groups. The Zn and P tetrahedra are bridged by the Ca atoms to form the novel two-dimensional layer structure shown in Figure 2. All the phosphite oxygen atoms interact with Ca except O(2), which bridges only P(1) and Zn. Of the remaining five, four are triply bridging, coordinating either to Zn and Ca (O(1), O(4), and O(5)) or to two Ca atoms (O(8)), while O(3) is doubly bridging, linking just P(2) and Ca. Thus the phosphite groups both chelate and bridge Ca while only bridging Zn. The Ca atoms sit in a distorted square antiprism (Figure 1) consisting of six phosphite oxygen atoms and two coordinated water molecules. There are six short Ca–O distances ranging from 2.376 (5) to 2.452 (6) Å and two long distances of 2.722 (6) and 2.984 (7) Å. The bonds to the water molecules (atoms O(6) and O(7)) are among the shorter distances. This type of 8-fold coordination for Ca is also found in phosphates such as $\text{Ca}(\text{H}_2\text{PO}_4)_2\cdot\text{H}_2\text{O}$ ¹⁴ ($d_{\text{Ca-O}} = 2.30\text{--}2.74 \text{ \AA}$). In the best known calcium-containing phosphates, the apatite family, Ca takes a 9-fold coordination, again with a wide range (ca. 2.30–3.00 Å) of Ca–O distances.¹⁵

The most interesting features of this material are the lamellar structure and the presence of the interlayer region, which is lined with the hydrogen atoms of the phosphite groups and coordinated water molecules. There are no apparent hydrogen-bonding interactions between the layers. As the calcium ions are an integral part of the layers, we would not expect them to be active with respect to ion exchange. However, the protons on the oxygen atoms bound to the electropositive Ca^{2+} ions may be somewhat acidic and thus may be mobile either in the solid state or in contact with aqueous solution (in which the compound is insoluble). The chemical and physical properties of this material are currently under investigation.

Given the structural relationship of the phosphite group to the phosphonates, in which the H atom is replaced by an organic R group, this compound can also serve as a model for new classes of layered phosphonates of the type reported recently by Mallouk^{6,7}

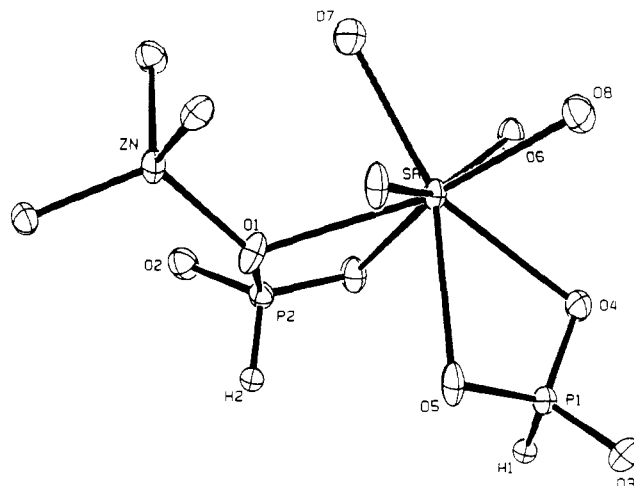


Figure 3. Connectivity of the polyhedra and atom-labeling scheme in $\text{ZnSr}(\text{HPO}_3)_2(\text{H}_2\text{O})_2$.

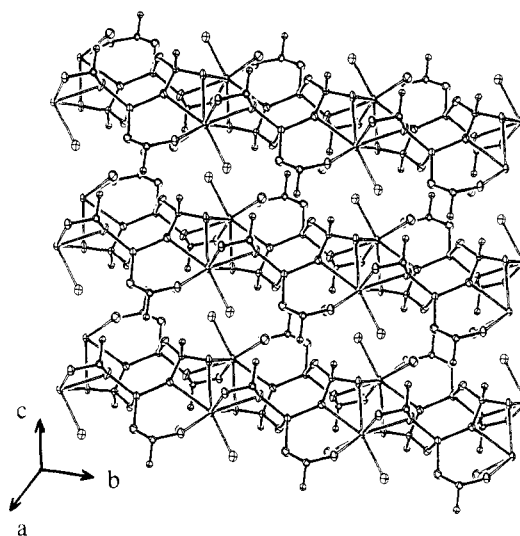


Figure 4. Edge-on view of the layers in $\text{ZnSr}(\text{HPO}_3)_2(\text{H}_2\text{O})_2$. Bonds to Zn and P are solid black, while those to Sr are hollow.

and by us.⁸ These materials contain $\text{M-O}_3\text{P}$ layers propped apart by the R groups, which are directed into the interlayer region.

$\text{ZnSr}(\text{HPO}_3)_2(\text{H}_2\text{O})_2$. As the chemical behavior of Sr is very similar to that of Ca, it was of interest to prepare the corresponding strontium zinc phosphite. The resultant compound has the same formula but a layered structure different from that of the calcium zinc phosphite. As shown in Figure 3 and Table III, the Zn coordination is again a nearly regular tetrahedron of oxygen atoms from four different phosphite groups. The Sr atoms are in an irregular 8-fold coordination that is intermediate between a square antiprism and a dodecahedron. As for Ca, the Sr coordination sphere contains six phosphite oxygen atoms and two coordinated water molecules (O(7) and O(8)). The Sr–O distances (2.533 (4)–2.760 (5) Å) are more regular than the Ca–O distances and are in good agreement with reported values in strontium phosphates.¹⁶ As in the Ca compound, the phosphite groups both chelate and bridge Sr while only bridging Zn; however, here the pattern is different. Only four of the six independent phosphite oxygen atoms are bridged by the Sr atom. All of these are 3-coordinate: O(5) and O(6) bridge two Sr atoms while O(1) and O(4) coordinate to both Zn and Sr. Atoms O(2) and O(3) are 2-coordinate, bridging between Zn and P(2) and P(1), respectively. This change in connectivity alters the layers and thus the nature of the void in the Sr compound. As may be seen in Figure 4, one of the phosphite groups juts out into the interlayer

(14) MacLennan, G.; Bevers, C. *Acta Crystallogr.* **1956**, *9*, 187–190.

(15) Posner, A.; Perloff, A.; Diorio, A. *Acta Crystallogr.* **1958**, *11*, 308–309.

(16) Boudjada, A.; Masse, R.; Guitel, J. *Acta Crystallogr., Sect. B* **1978**, *34*, 2692–2695.

Table II. Positional Parameters and Equivalent Isotropic Thermal Parameters

atom	x	y	z	$B_{eq},^a \text{ \AA}^2$
ZnCa(HPO₃)₂(H₂O)₂				
Zn	0.3768 (1)	0.0734 (1)	0.85887 (6)	1.25 (4)
Ca	0.4815 (2)	0.5567 (2)	0.8679 (1)	1.16 (6)
P(1)	0.2695 (3)	0.8035 (2)	1.0067 (1)	1.00 (7)
P(2)	0.0824 (3)	0.3747 (2)	0.8186 (1)	0.97 (7)
O(1)	0.2440 (7)	0.2862 (6)	0.8819 (3)	1.4 (2)
O(2)	0.6332 (7)	0.0703 (6)	0.9213 (4)	1.4 (2)
O(3)	0.5290 (7)	0.7595 (7)	0.7501 (4)	1.6 (2)
O(4)	0.261 (1)	-0.1311 (7)	0.9072 (4)	2.4 (2)
O(5)	0.3284 (7)	0.0282 (6)	0.7250 (3)	1.3 (2)
O(6)	0.7468 (7)	0.7286 (7)	0.9248 (3)	1.6 (2)
O(7)	0.5742 (8)	0.3533 (8)	0.7569 (4)	2.2 (2)
O(8)	0.6448 (8)	0.3753 (6)	0.9866 (4)	1.7 (2)
H(1)	0.1189	0.8015	1.0207	1.2
H(2)	-0.0090	0.4090	0.8714	1.1
H(3)	0.7608	0.7121	0.9768	1.9
H(4)	0.8407	0.7208	0.8962	1.9
H(5)	0.7101	0.3231	0.7415	2.6
ZnSr(HPO₃)₂(H₂O)₂				
Sr	0.28416 (8)	0.02229 (8)	0.6076 (1)	1.21 (2)
Zn	0.2768 (1)	-0.4852 (1)	0.5746 (1)	1.43 (3)
P(1)	0.3293 (2)	0.2217 (2)	0.2660 (3)	1.15 (5)
P(2)	0.0199 (2)	-0.3264 (2)	0.2755 (3)	1.22 (5)
O(1)	0.2146 (6)	-0.3180 (6)	0.4196 (8)	1.9 (2)
O(2)	-0.1248 (6)	-0.4912 (6)	0.2628 (7)	1.8 (2)
O(3)	0.4692 (6)	0.3700 (6)	0.2393 (7)	1.7 (2)
O(4)	0.2654 (7)	0.2851 (6)	0.4342 (7)	1.9 (2)
O(5)	0.3973 (6)	0.0574 (6)	0.2957 (8)	1.9 (2)
O(6)	0.0296 (6)	0.1555 (6)	0.6729 (7)	1.6 (2)
O(7)	0.2248 (8)	-0.1339 (7)	0.8679 (8)	2.4 (2)
O(8)	0.5048 (7)	0.2960 (7)	0.8674 (8)	2.4 (2)
H(1)	0.1993	0.1788	0.1152	1.3
H(2)	0.0453	-0.3432	0.1167	1.4
Zn(O₂PHC₆H₅)₂				
Zn	1/2	0.0588 (2)	1/4	1.8 (1)
P	0.6149 (2)	-0.1410 (3)	0.5212 (4)	2.3 (2)
O(1)	0.5943 (5)	-0.0341 (9)	0.407 (1)	3.8 (4)
O(2)	0.5553 (5)	0.1618 (8)	0.129 (1)	2.5 (4)
C(1)	0.7296 (8)	-0.131 (1)	0.656 (1)	2.0 (5)
C(2)	0.7870 (9)	-0.040 (1)	0.639 (2)	3.0 (7)
C(3)	0.8756 (9)	-0.036 (1)	0.748 (2)	3.7 (7)
C(4)	0.908 (1)	-0.121 (2)	0.870 (2)	3.9 (7)
C(5)	0.853 (1)	-0.211 (2)	0.891 (2)	3.7 (7)
C(6)	0.7647 (9)	-0.214 (1)	0.784 (2)	2.8 (6)
H(1)	0.605 (7)	-0.23 (1)	0.41 (1)	2.8
H(2)	0.770 (9)	0.01 (1)	0.59 (2)	3.2
H(3)	0.907 (8)	0.02 (1)	0.73 (2)	4.4
H(4)	0.961 (8)	-0.11 (1)	0.93 (2)	4.5
H(5)	0.874 (8)	-0.28 (1)	0.96 (2)	4.5
H(6)	0.729 (7)	-0.27 (1)	0.79 (1)	3.3

$$^a B_{eq} = \frac{4}{3}[a^2\beta_{11} + b^2\beta_{22} + c^2\beta_{33} + (2ab \cos \gamma)\beta_{12} + (2ac \cos \beta)\beta_{13} + (2bc \cos \alpha)\beta_{23}]$$

region, appearing to partition the gap into channels parallel to [100]. The effect of this different topography is evident in the repeat distances between the layers in the two compounds. In the Ca phase, in which the layers are parallel to (101), it is ca. 6.05 Å, while, in the Sr compound (layers parallel to (110)), it is 7.49 Å.

We have now synthesized from aqueous solution a series of zinc phosphites containing alkali or alkaline-earth-metal ions. The structures of the phases $Zn_3Na_2(HPO_3)_4$, $Zn_3K_2(HPO_3)_4$, and $Zn_3Ba(HPO_3)_4(H_2O)_6$ were described in an earlier report.³ The results for these compounds, together with $ZnCa(HPO_3)_2(H_2O)_2$ and $ZnSr(HPO_3)_2(H_2O)_2$, are summarized in Table IV in terms of the coordination behavior of the group I and II metal ions. As expected, the coordination numbers (CN) increase with ionic radius and charge. This increase is accomplished by inclusion of increasing numbers of water molecules in the coordination sphere. Also, the manner in which the ions bridge the phosphite groups changes with ionic size. Thus, though the Na^+ and K^+ compounds have the same composition, they have different

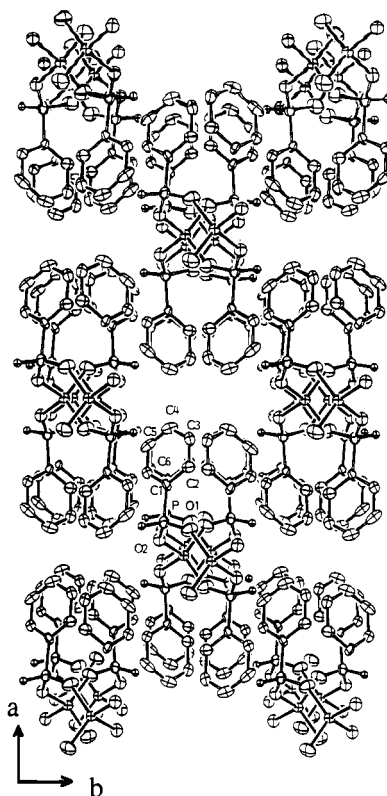


Figure 5. Perspective view of the $Zn(O_2PHC_6H_5)_2$ structure along [001] showing the atom-labeling scheme. Phenyl hydrogen atoms have been omitted. Bonds to Zn are shown in solid black.

structures, with the $Zn_3K_2(HPO_3)_4$ framework possessing small tunnels that are absent from the $Zn_3Na_2(HPO_3)_4$ structure. The reason for this difference is evident in the M–O bond distances in Table IV, which correspond to the differences in ionic radii of Na^+ and K^+ . It is perhaps surprising that Ca^{2+} and Sr^{2+} , which are much closer in size, should also yield heteromorphic structures. Here, too, the difference in ionic radii is reflected in the M–O distances and the resulting polyhedral connectivities.

On going from group I to group II, there is a clear change in behavior as well. Whereas the compounds containing the monovalent ions have compact three-dimensional structures with no water, those of the divalent ions are two-dimensional (i.e., layered) with large open spaces lined with water molecules. This trend continues with the Ba^{2+} structure, which has a pattern of crisscrossing layers that form large channels. That the divalent ions form more open structures may be due in part to their tendency to favor chelation by the phosphite ions and inclusion of water molecules in the coordination sphere.

It is clear that in the Zn–M– HPO_3 (M = group I or II metal) system, the M ion is the key factor in determining the type of structure that crystallizes from aqueous solution. In each case, the tetrahedral HPO_3^{2-} ions are bridged by the Zn^{2+} ions so as to give zinc a regular tetrahedral coordination. It is the manner in which the M ion bridges these tetrahedra that fixes the nature of the framework. These results suggest a great diversity of structures in as yet unexplored systems. Moreover, as the phosphite ion represents a rigid building block, it should be possible to predict the types of structures that will form primarily from a knowledge of the coordination behavior of the metal ions in similar systems.

$Zn(O_2PHC_6H_5)_2$. The structure, shown in Figure 5, consists of isolated $(Zn(O_2PHC_6H_5)_2)_n$ chains running parallel to the c axis. The phosphonate groups bridge alternate zinc atoms in a zigzag pattern in the b–c plane. The zinc coordination is tetrahedral with regular bond distances and angles. Each of the oxygen atoms in the zinc coordination sphere is from a different phosphonate group, and so, there is no chelation to zinc in this compound. The oxygen atoms are 2-coordinate, bridging just Zn and P. As might be expected, the O(1)–P–O(2) angle has opened

Table III. Selected Interatomic Distances (Å) and Angles (deg)

ZnCa(HPO ₃) ₂ (H ₂ O) ₂							
Zn-O(2)	1.934 (5)	P(1)-O(8)	1.515 (5)	P(2)-O(5)	1.525 (5)	Ca-O(7)	2.405 (6)
Zn-O(1)	1.955 (5)	P(1)-O(4)	1.521 (6)	P(2)-O(1)	1.540 (5)	Ca-O(5)	2.447 (5)
Zn-O(5)	1.957 (5)	P(1)-O(2)	1.531 (5)	Ca-O(6)	2.376 (5)	Ca-O(8)	2.452 (6)
Zn-O(4)	1.960 (6)	P(2)-H(2)	1.098	Ca-O(3)	2.378 (5)	Ca-O(1)	2.722 (6)
P(1)-H(1)	1.118	P(2)-O(3)	1.490 (5)	Ca-O(8)	2.405 (5)	Ca-O(4)	2.984 (7)
O(2)-Zn-O(1)	112.4 (2)	H(2)-P(2)-O(3)	107.26	O(6)-Ca-O(4)	83.8 (2)	O(8)-Ca-O(4)	124.0 (2)
O(2)-Zn-O(5)	119.9 (2)	H(2)-P(2)-O(5)	114.49	O(3)-Ca-O(8)	143.2 (2)	O(7)-Ca-O(5)	83.0 (2)
O(2)-Zn-O(4)	103.8 (2)	H(2)-P(2)-O(1)	99.21	O(3)-Ca-O(7)	83.1 (2)	O(7)-Ca-O(8)	151.4 (2)
O(1)-Zn-O(5)	107.0 (2)	O(3)-P(2)-O(5)	114.1 (3)	O(3)-Ca-O(5)	82.3 (2)	O(7)-Ca-O(1)	76.7 (2)
O(1)-Zn-O(4)	112.9 (3)	O(3)-P(2)-O(1)	115.1 (3)	O(3)-Ca-O(8)	125.1 (2)	O(7)-Ca-O(4)	149.0 (2)
O(5)-Zn-O(4)	100.3 (2)	O(5)-P(2)-O(1)	106.0 (3)	O(3)-Ca-O(1)	135.3 (2)	O(5)-Ca-O(8)	95.0 (2)
H(1)-P(1)-O(8)	111.39	O(6)-Ca-O(3)	72.3 (2)	O(3)-Ca-O(4)	74.0 (2)	O(5)-Ca-O(1)	56.2 (2)
H(1)-P(1)-O(4)	104.64	O(6)-Ca-O(8)	77.9 (2)	O(8)-Ca-O(7)	86.8 (2)	O(5)-Ca-O(4)	73.6 (2)
H(1)-P(1)-O(2)	104.38	O(6)-Ca-O(7)	109.1 (2)	O(8)-Ca-O(5)	131.4 (2)	O(8)-Ca-O(1)	78.6 (2)
O(8)-P(1)-O(4)	109.5 (3)	O(8)-Ca-O(5)	149.9 (2)	O(8)-Ca-O(8)	73.1 (2)	O(8)-Ca-O(4)	53.2 (2)
O(8)-P(1)-O(2)	113.5 (3)	O(6)-Ca-O(8)	86.8 (2)	O(8)-Ca-O(1)	75.2 (2)	O(1)-Ca-O(4)	105.4 (2)
O(4)-P(1)-O(2)	113.0 (3)	O(6)-Ca-O(1)	152.1 (2)				
ZnSr(HPO ₃) ₂ (H ₂ O) ₂							
Zn-O(4)	1.924 (5)	P(1)-O(5)	1.521 (5)	P(2)-O(2)	1.530 (5)	Sr-O(7)	2.580 (5)
Zn-O(1)	1.935 (5)	P(1)-O(4)	1.526 (5)	P(2)-O(1)	1.538 (5)	Sr-O(6)	2.626 (5)
Zn-O(2)	1.937 (5)	P(1)-O(3)	1.533 (5)	Sr-O(6)	2.533 (4)	Sr-O(4)	2.639 (5)
Zn-O(3)	1.965 (5)	P(2)-H(2)	1.248	Sr-O(5)	2.571 (5)	Sr-O(1)	2.709 (5)
P(1)-H(1)	1.200	P(2)-O(6)	1.502 (5)	Sr-O(8)	2.572 (5)	Sr-O(5)	2.760 (5)
O(4)-Zn-O(1)	116.0 (2)	H(2)-P(2)-O(6)	110.50	O(6)-Sr-O(5)	122.7 (1)	O(8)-Sr-O(5)	101.2 (2)
O(4)-Zn-O(2)	109.2 (2)	H(2)-P(2)-O(2)	107.50	O(5)-Sr-O(8)	76.7 (2)	O(7)-Sr-O(6)	95.7 (2)
O(4)-Zn-O(3)	111.4 (2)	H(2)-P(2)-O(1)	102.87	O(5)-Sr-O(7)	85.3 (2)	O(7)-Sr-O(4)	150.7 (2)
O(1)-Zn-O(2)	111.3 (2)	O(6)-P(2)-O(2)	115.4 (3)	O(5)-Sr-O(6)	127.9 (1)	O(7)-Sr-O(1)	79.6 (2)
O(1)-Zn-O(3)	104.4 (2)	O(6)-P(2)-O(1)	108.7 (3)	O(5)-Sr-O(4)	115.8 (2)	O(7)-Sr-O(5)	154.9 (1)
O(2)-Zn-O(3)	103.8 (2)	O(2)-P(2)-O(1)	111.2 (3)	O(5)-Sr-O(1)	74.2 (1)	O(6)-Sr-O(4)	87.2 (2)
H(1)-P(1)-O(5)	106.48	O(6)-Sr-O(5)	154.5 (2)	O(5)-Sr-O(5)	77.3 (2)	O(6)-Sr-O(1)	55.1 (1)
H(1)-P(1)-O(4)	110.43	O(6)-Sr-O(8)	83.4 (2)	O(8)-Sr-O(7)	91.9 (2)	O(6)-Sr-O(5)	81.5 (1)
H(1)-P(1)-O(3)	104.49	O(6)-Sr-O(7)	79.7 (2)	O(8)-Sr-O(6)	154.7 (2)	O(4)-Sr-O(1)	124.3 (2)
O(5)-P(1)-O(4)	108.2 (3)	O(6)-Sr-O(6)	74.4 (2)	O(8)-Sr-O(4)	74.8 (2)	O(4)-Sr-O(5)	54.4 (1)
O(5)-P(1)-O(3)	115.6 (3)	O(6)-Sr-O(4)	73.0 (1)	O(8)-Sr-O(1)	150.2 (2)	O(1)-Sr-O(5)	78.5 (1)
O(4)-P(1)-O(3)	111.5 (3)	O(6)-Sr-O(1)	122.3 (1)				
Zn(O ₂ PHC ₆ H ₅) ₂							
Zn-O(2)	1.916 (8)	P-O(2)	1.510 (9)	C(1)-C(2)	1.39 (2)	C(4)-C(5)	1.38 (2)
Zn-O(1)	1.921 (8)	P-C(1)	1.79 (1)	C(2)-C(3)	1.39 (2)	C(5)-C(6)	1.38 (2)
P-O(1)	1.49 (1)	C(1)-C(6)	1.38 (2)	C(3)-C(4)	1.35 (2)		
O(2)-Zn-O(2)	106.2 (5)	O(1)-P-O(2)	116.7 (5)	C(6)-C(1)-C(2)	117 (1)	C(3)-C(4)-C(5)	120 (1)
O(2)-Zn-O(1)	107.0 (3)	O(1)-P-C(1)	107.9 (6)	C(3)-C(2)-C(1)	120 (1)	C(6)-C(5)-C(4)	119 (1)
O(2)-Zn-O(1)	110.8 (4)	O(2)-P-C(1)	110.1 (5)	C(4)-C(3)-C(2)	121 (1)	C(5)-C(6)-C(1)	122 (1)
O(1)-Zn-O(1)	114.7 (6)						

Table IV. Coordination Environments of Alkali- and Alkaline-Earth-Metal Ions in Zinc Phosphites^a

ion	radius, Å ^b	CN	bond dist to O, Å	no. of water molecules in coordn sphere
Na ⁺	1.02	6	2.389 (8)-2.904 (7)	0
K ⁺	1.38	7	2.652 (8)-3.262 (7)	0
Ca ²⁺	1.00	8	2.376 (5)-2.984 (7)	2
Sr ²⁺	1.18	8	2.533 (4)-2.760 (5)	2
Ba ²⁺	1.38	12	2.876 (4)-3.053 (6)	8

^aNa⁺, K⁺, Ba²⁺: ref 3. Ca²⁺, Sr²⁺: this work. ^bReference 20.

about 7° from the ideal tetrahedral angle to accommodate the bridging arrangement.

The chains pack so as to create a face-centered array in the *a-b* plane. The closest nonbonded contacts between the phenyl groups are 2.8 (2) Å (H(3)-H(3')) within a chain and 2.8 (3) Å (H(4)-H(4')) between neighboring chains. The shortest contacts within the parallel sets of rings along the chains are nearly 4 Å (C(2)-C(6) = 3.83 (2) Å).

The polymeric nature of the Zn(O₂PHC₆H₅)₂ structure is, as it turns out, typical of phosphinate salts of divalent transition metals, which were widely studied in the early 1970s as so-called inorganic coordination polymers.¹⁷⁻¹⁹ Thus, Zn(O₂P(*n*-

C₄H₉)(C₆H₅)₂)₂¹⁸ also possesses infinite chains of tetrahedral zinc atoms bridged by the phosphinate groups, and Pb(O₂P(C₆H₅)₂)₂¹⁹ has a polymeric structure very similar to that of the present compound, except that the lead coordination is distorted to a trigonal bipyramid by a lone electron pair that occupies an equatorial site. Analogous materials have been reported for most of the first-row transition metals;¹⁷ however structural data on these compounds are lacking. The Zn(O₂PHC₆H₅)₂ structure is distinguished from the reported structures in that it is based on a mono- rather than a bis-substituted phosphinate. The absence of the extra R group leads, as expected, to a more compact packing of the chains.

The phosphinate structures may be contrasted with those of the divalent metal phosphonates.⁵⁻⁸ For example, zinc phenylphosphonate, Zn(O₃PC₆H₅)₂·H₂O,^{7,8} has a layered structure in which the Zn atoms are octahedrally coordinated by the phosphonate groups (the water molecule completes the octahedron) in both chelating and bridging modes, with the phenyl groups directed into the gap between these Zn-O₃P layers. Thus, the dimensionality of these simple materials is a direct function of the number of oxygen atoms available for bonding to the metal

(18) Giordano, F.; Randaccio, L.; Ripamonti, A. *Acta Crystallogr., Sect. B* **1969**, *25*, 1057-1065.

(19) Colamarino, P.; Orioli, P.; Benzinger, W.; Gillman, H. *Inorg. Chem.* **1976**, *15*, 800-804.

(20) Shannon, R. D. *Acta Crystallogr., Sect. A* **1976**, *32*, 751-767.

(17) Gillman, H. *Inorg. Chem.* **1974**, *13*, 1921-1924.

atoms. These results suggest that it should be possible to prepare new materials with different structures from mixed phosphate-phosphinate or phosphite systems. This work is in progress.

Acknowledgment. We gratefully acknowledge support for this work by the Robert A. Welch Foundation under Grant No. A673.

The single-crystal diffractometer was purchased under DOD Grant No. N-00014-86-G-0194.

Supplementary Material Available: Table SI, giving experimental crystallographic details and anisotropic thermal parameters (4 pages); Table SII, listing calculated and observed structure amplitudes (29 pages). Ordering information is given on any current masthead page.

Contribution from the Dipartimento di Chimica, Università di Firenze, Via Maragliano 75/77, 50144 Firenze, Italy, Laboratoire de Chimie des Métaux de Transition, Université Pierre et Marie Curie, 75230 Paris, France, and Departament de Química Inorgànica, Facultat de Química, Universitat de València, C/Dr. Moliner 50, Burjassot, 46100 València, Spain

Oxalato and Squarate Ligands in Nickel(II) Complexes of Tetraazacycloalkanes. Solution and Solid-State Studies. Crystal and Molecular Structures of (μ -Oxalato)bis[(1,7-dimethyl-1,4,7,10-tetraazacyclododecane)nickel(II)] Perchlorate Dihydrate and of Bis[diaquo(1,4,7,10-tetraazacyclododecane)nickel(II)] Squarate Diperchlorate

Andrea Bencini,^{1a} Antonio Bianchi,^{*1a} Enrique Garcia-España,^{*1b} Yves Jeannin,^{1c} Miguel Julve,^{*1b} Victor Marcelino,^{1b} and Michèle Philoche-Levisalles^{1c}

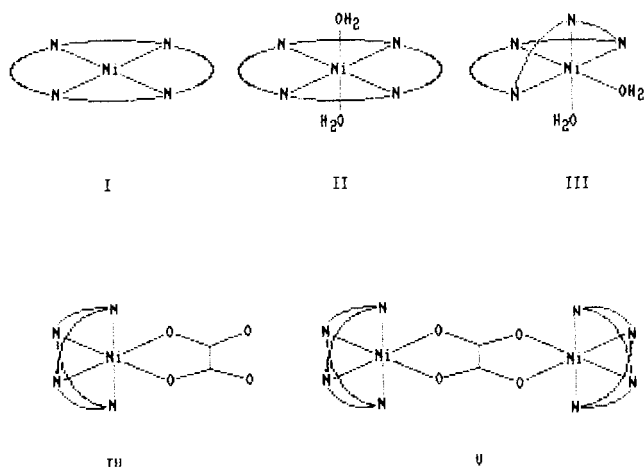
Received May 12, 1989

Three new nickel(II) complexes of formula $[\text{Ni}_2(\text{Me}_2\text{cyclen})_2\text{ox}](\text{ClO}_4)_2 \cdot 2\text{H}_2\text{O}$ (1), $[\text{Ni}_2(\text{cyclen})_2\text{ox}](\text{NO}_3)_2$ (2), and $[\text{Ni}(\text{cyclen})(\text{H}_2\text{O})_2](\text{C}_4\text{O}_4)(\text{ClO}_4)_2$ (3), where $\text{Me}_2\text{cyclen} = 1,7$ -dimethyl-1,4,7,10-tetraazacyclododecane, $\text{cyclen} = 1,4,7,10$ -tetraazacyclododecane, ox^{2-} = the oxalate anion, and $\text{C}_4\text{O}_4^{2-}$ = the dianion of 3,4-dihydroxy-3-cyclobutene-1,2-dione (squarate), have been synthesized. The crystal and molecular structures of 1 and 3 have been solved at 298 K by single-crystal X-ray analyses. 1 crystallizes in the monoclinic system, space group $P2_1/n$, with $a = 22.815$ (15) Å, $b = 10.713$ (1) Å, $c = 7.506$ (3) Å, $\beta = 97.85$ (3)°, $Z = 2$, and $R = 0.0415$. 3 crystallizes in the orthorhombic system, space group $P2_1cn$, with $a = 11.124$ (3) Å, $b = 11.461$ (3) Å, $c = 5.735$ (6) Å, $Z = 4$, and $R = 0.0345$. The structure of 1 consists of centrosymmetrical μ -oxalato-bridged nickel(II) binuclear units $[\text{Ni}_2(\text{Me}_2\text{cyclen})_2\text{ox}]^{2+}$ with noncoordinated perchlorate anions and water molecules. The tetraazamacrocycle adopts a folded conformation around the nickel atom, which is 6-coordinated in an octahedral distorted arrangement: the Ni-N distances are in the range 2.050 (2)–2.154 (3) Å, and the Ni-O(ox) distances are 2.095 (2) and 2.102 (2) Å. The oxalate ion acts as a bis-bidentate ligand between two nickel(II) ions. The structure of 3 is made up of $[\text{Ni}(\text{cyclen})(\text{H}_2\text{O})_2]^{2+}$ units and noncoordinated squarate and perchlorate anions. The tetraazamacrocycle adopts a folded conformation to produce a cis-pseudooctahedral geometry at each nickel atom. The configuration of the four nitrogen atoms is such that the hydrogen atoms attached to them are on the same side with respect to the idealized macrocyclic plane. Coordinated water molecules and squarate oxygen atoms are linked by hydrogen bonds. Intramolecular antiferromagnetic spin-exchange coupling between the two nickel(II) ions is observed for complexes 1 ($J = -34 \text{ cm}^{-1}$; $g = 2.30$) and 2 ($J = -35 \text{ cm}^{-1}$; $g = 2.15$) (J being the parameter of the exchange Hamiltonian $\hat{H} = -J\hat{S}_A\hat{S}_B$). The thermodynamic parameters of the equilibrium $[\text{Ni}(\text{L})]^{2+} + \text{ox}^{2-} = [\text{Ni}(\text{L})\text{ox}]$ where L = cyclam, cyclen, and Me_2cyclen have been determined by potentiometric and microcalorimetric measurements in aqueous solution at 25 °C in 0.1 mol dm^{-3} KNO_3 . The values of ΔG° found for the addition of the oxalate anion to $[\text{Ni}(\text{cyclen})]^{2+}$ and $[\text{Ni}(\text{Me}_2\text{cyclen})]^{2+}$ are equal within experimental error ($\Delta G^\circ = -5.6$ (1) and -5.7 (1) kcal mol^{-1} , respectively). A greater enthalpy of reaction has been found for $[\text{Ni}(\text{Me}_2\text{cyclen})]^{2+}$ ($\Delta H^\circ = -2.9$ (1) kcal mol^{-1}) than for $[\text{Ni}(\text{cyclen})]^{2+}$ ($\Delta H^\circ = -2.4$ (1) kcal mol^{-1}). The addition of oxalate to $[\text{Ni}(\text{cyclam})]^{2+}$ (69% square, 29% *trans*-diaquo, 2% *cis*-diaquo forms) is an enthalpy-driven reaction ($\Delta G^\circ = -3.8$ (1) kcal mol^{-1} and $\Delta H^\circ = -3.8$ (1) kcal mol^{-1}). From these values, the thermodynamic parameters for the reaction of oxalate with each one of the three forms have been calculated and discussed.

Introduction

In a recent paper,² we have reported the synthesis, crystal structure, and magnetic properties of the mixed-ligand complex $[\text{Ni}_2(\text{cyclam})_2\text{ox}](\text{NO}_3)_2$ (cyclam = 1,4,8,11-tetraazacyclotetradecane and ox^{2-} = oxalate anion). In this complex, oxalate acts as a bis-bidentate ligand bridging two $[\text{Ni}(\text{cyclam})]^{2+}$ units. In the same paper, we have also reported the equilibrium constants for the reactions $[\text{Ni}(\text{cyclam})]^{2+} + \text{ox}^{2-} = [\text{Ni}(\text{cyclam})\text{ox}]$ and $[\text{Ni}(\text{cyclam})\text{ox}] + [\text{Ni}(\text{cyclam})]^{2+} = [\text{Ni}_2(\text{cyclam})_2\text{ox}]^{2+}$. Aqueous solutions of $[\text{Ni}(\text{cyclam})]^{2+}$ are composed by an equilibrium mixture involving a square diamagnetic and two octahedral paramagnetic (both *cis*- and *trans*-diaquo) species (Chart I), the *cis*-diaquo complex being present in a very low percentage.³ The oxalate anion can coordinate to $[\text{Ni}(\text{cyclam})]^{2+}$ in a bidentate fashion when the tetraazamacrocyclic ligand is arranged in a folded conformation (Chart I, drawing IV), so that only the *cis*-diaquo

Chart I



form (Chart I, drawing III) exhibits the right conformation to allow such a coordination. The formation of the oxalato-bridged complex $[\text{Ni}_2(\text{cyclam})_2\text{ox}]^{2+}$ gives rise, owing to the particular

(1) (a) Università di Firenze. (b) Universitat de València. (c) Université Pierre et Marie Curie.
 (2) Battaglia, L. P.; Bianchi, A.; Bonamartini Corradi, A.; Garcia-España, E.; Julve, M.; Micheloni, M. *Inorg. Chem.* 1988, 27, 4174.
 (3) Billo, E. J. *Inorg. Chem.* 1984, 23, 2223.